



遼寧師範大學
Liaoning Normal University

Searching for axion-like particles at future electron-positron colliders

Shuo Yang

(Liaoning Normal University)

in collaboration with

Huaying Zhang, Chong-Xing Yue and Yu-Chen Guo

arXiv: 2103.05218, accepted by PRD

The 2021 International Workshop on the High Energy Circular
Electron Positron Collider
November 8-12, 2021, Nanjing

Outline

- 1. Introduction to axion and axion-like particles.
- 2. General effective Lagrangian of ALPs
- 3. ALPs searches at colliders
- 4. Searching for ALPs at future e^+e^- colliders via light-by-light scattering
- 5. Summary

Introduction to axion and axion-like particles.

- The discovery of Higgs bring us into new territory of spin-0 particles.
- Axion have been postulated to address the strong CP problem, which is the pNGB associated to Peccei-Quinn symmetry, a global U(1). $m_a \sim m_\pi f_\pi / f_a$
- Many extensions of SM feature one or several spontaneously broken global U(1) symmetries, thus predicting the existence of axion-like particles (ALPs).
- ALPs: No direct relation between coupling and mass.

General effective Lagrangian of ALPs

bottom-up view

SMEFT $\mathcal{L} = \mathcal{L}_0 + \sum_i \frac{c_i}{\Lambda^{d-4}} \mathbf{O}_i$

Building Blocks:

SM fields: $B_{\mu\nu}, W_{\mu\nu}, G_{\mu\nu}$

EW scalar doublet: $\Phi(x) = \frac{v + h(x)}{\sqrt{2}} e^{i\vec{\pi}\vec{\sigma}/v}$

New pseudoscalar GB: $\frac{\partial_\mu a}{f_a}$

General effective Lagrangian of ALPs

Linear Effective Lagrangian

NLO bosonic operators

$$\mathcal{O}_{\tilde{B}} = -B_{\mu\nu} \tilde{B}^{\mu\nu} \frac{a}{f_a}$$

$$\mathcal{O}_{\tilde{G}} = -G_{\mu\nu}^a \tilde{G}^{a\mu\nu} \frac{a}{f_a}$$

$$\mathcal{O}_{\tilde{W}} = -W_{\mu\nu} \tilde{W}^{\mu\nu} \frac{a}{f_a}$$

$$\mathcal{O}_{a\Phi} = i(\Phi^\dagger \overleftrightarrow{D}_\mu \Phi) \frac{\partial^\mu a}{f_a}$$

$$\mathcal{L}_{\text{eff}}^{D \leq 5} = \frac{1}{2} (\partial_\mu a) (\partial^\mu a) - \frac{M_a^2}{2} a^2 + \frac{\partial^\mu a}{\Lambda} \sum_F \bar{\psi}_F C_F \gamma_\mu \psi_F$$

$$+ g_s^2 C_{GG} \frac{a}{\Lambda} G_{\mu\nu}^A \tilde{G}^{\mu\nu,A} + g^2 C_{WW} \frac{a}{\Lambda} W_{\mu\nu}^A \tilde{W}^{\mu\nu,A} + g'^2 C_{BB} \frac{a}{\Lambda} B_{\mu\nu} \tilde{B}^{\mu\nu}$$

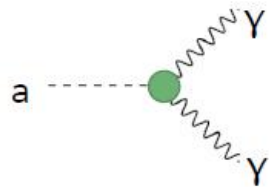
$$\mathcal{L}_{\text{eff}}^{D \geq 6} = \frac{c_{ah}}{f^2} (\partial_\mu a) (\partial^\mu a) \phi^\dagger \phi + \frac{c_{Zh}}{f^3} (\partial^\mu a) \left(\phi^\dagger i D_\mu \phi + \text{h.c.} \right) \phi^\dagger \phi + \dots$$

H. Georgi, D.B. Kaplan & L. Randall, PLB169(1986)73-78

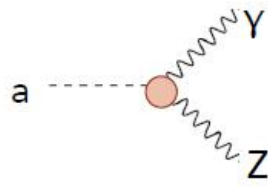
I. Brivio et al., EPJC77(2017),8,572 (Noliner Effective Lagrangian)

General effective Lagrangian of ALPs

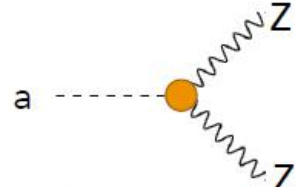
$$\frac{a}{f_a} \left(c_{\tilde{B}} B_{\mu\nu} \tilde{B}^{\mu\nu} + c_{\tilde{W}} W_{\mu\nu} \tilde{W}^{\mu\nu} \right)$$



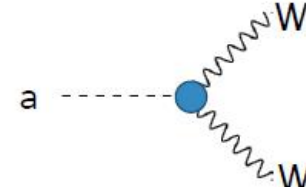
$$c_{\tilde{B}} c_{\theta}^2 + c_{\tilde{W}} s_{\theta}^2$$



$$\frac{s_{2\theta}}{2} (c_{\tilde{B}} - c_{\tilde{W}})$$



$$s_{\theta}^2 c_{\tilde{B}} + c_{\theta}^2 c_{\tilde{W}}$$

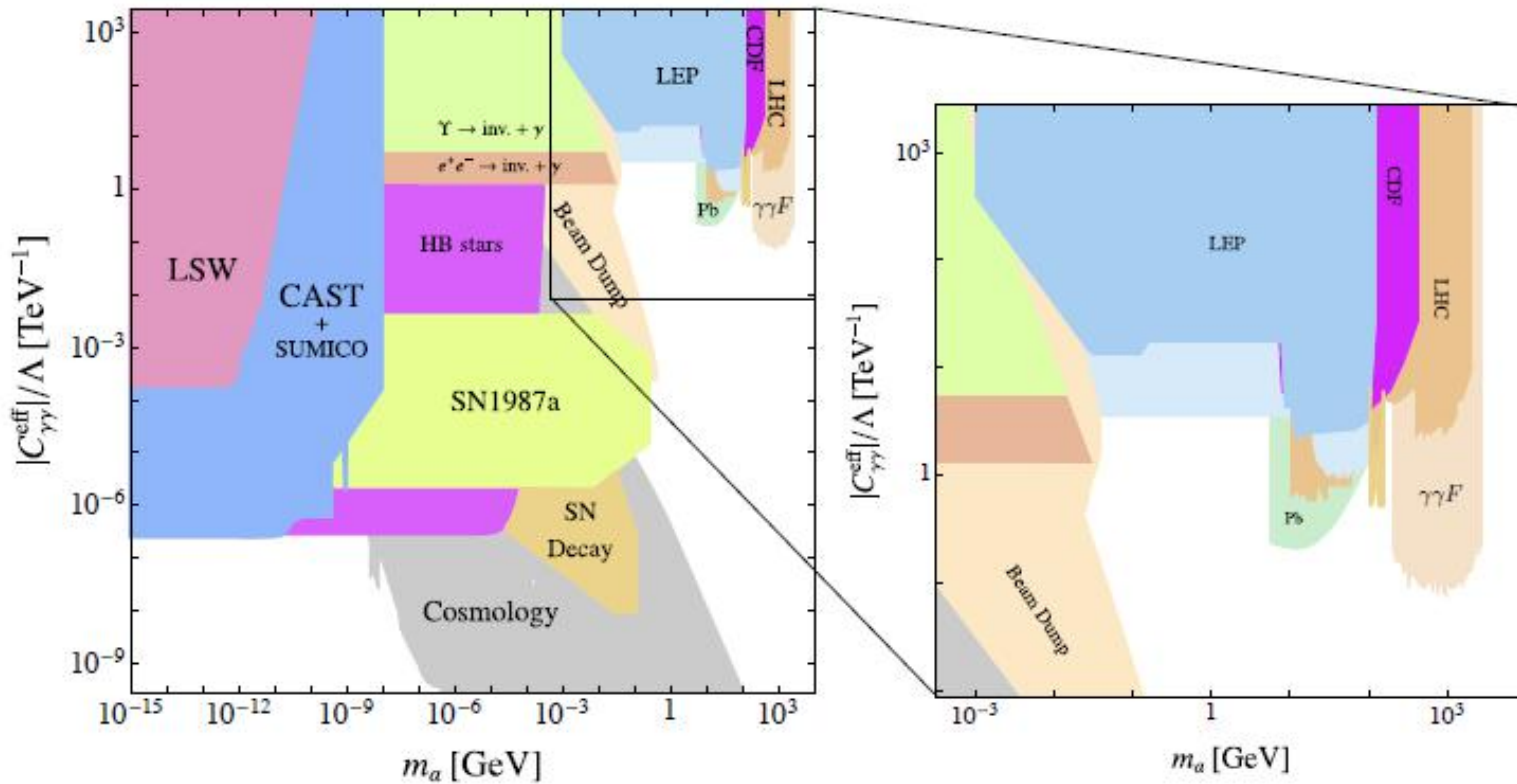


$$c_{\tilde{W}}$$

stolen from R.del Rey's talk

Constraints: di-photon coupling

M. Bauer et al., JHEP12(2017),044



1. For light ALPs (\ll MeV), cosmological and astrophysical measurements place very tight bounds on the coupling to photons.
2. For heavier ALPs, the limits are less stringent.

ALPs searches at colliders

Production modes

- Resonant production

$$gg \rightarrow a \quad \gamma\gamma \rightarrow a$$

$$e^+e^- \rightarrow a \quad \text{strongly suppressed}$$

- Associated production

$$pp \rightarrow aW^\pm \quad pp \rightarrow aZ(\gamma)$$

$$pp \rightarrow ah \quad pp \rightarrow t\bar{t}a \quad pp \rightarrow aW^\pm\gamma$$

$$e^+e^- \rightarrow aZ(\gamma) \quad e^+e^- \rightarrow ah$$

$$e^+e^- \rightarrow e^+e^-a \quad e^+e^- \rightarrow \nu\bar{\nu}a$$

- Exotic SM decays

$$h \rightarrow Za \quad h \rightarrow aa \quad Z \rightarrow a\gamma$$

- Other modes

Decay channels

- Stable ALPs $\sim \cancel{E}$

- Long-Lived ALPs with a Displaced-Vertex

- Short lived ALP

$$a \rightarrow \gamma\gamma \quad a \rightarrow \ell^+\ell^- \quad a \rightarrow jj$$

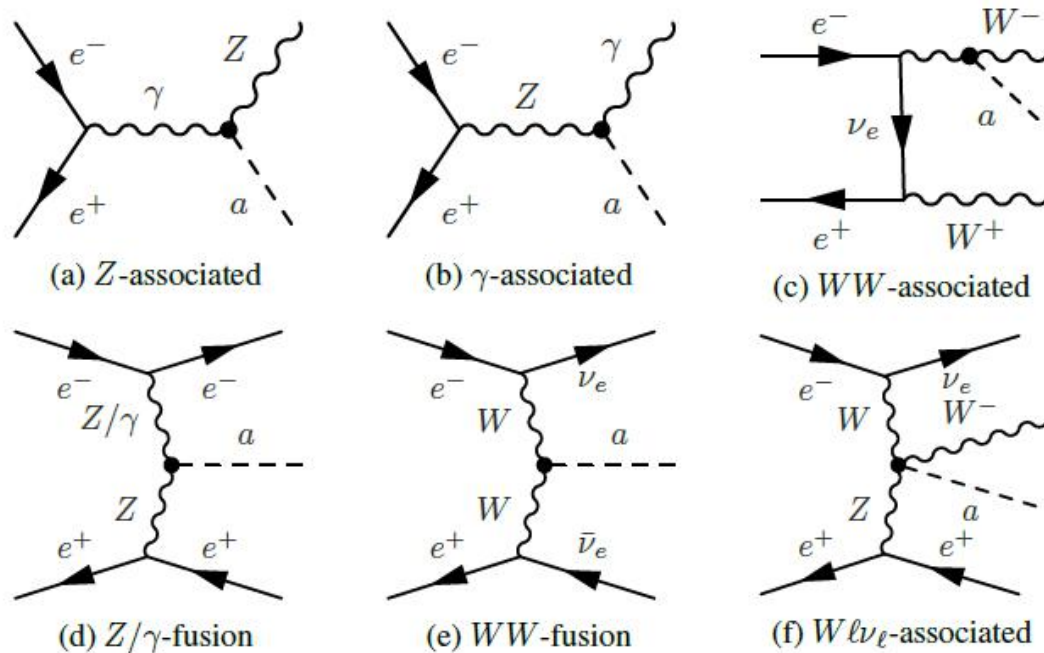
$$a \rightarrow b\bar{b} \quad a \rightarrow VV \quad a \rightarrow t\bar{t}$$

I.Brivio et al., EPJC77(2017),8,572

M.Bauer et al., EPJC79(2019),1,74

CERN Yellow Rep. Monogr. Vol. 3 (2018)

ALPs searches at e+e-colliders

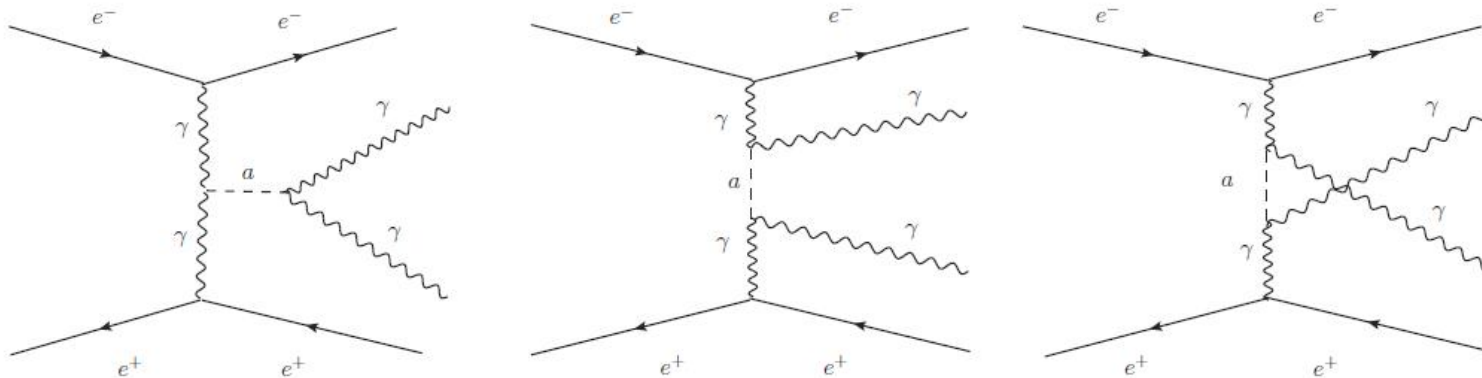


Respective Feynman diagrams for ALP production processed at e+e- colliders

Searching for ALPs at future e+e- colliders via light-by-light scattering

H-Y Zhang, C-X Yue, Y-C Guo and **SY**
arXiv: 2021.05218, accepted by PRD

- Using proton tagging technique, the LHC generally is more sensitive to the heavy ALP searched by LBL scattering than other processes. The CLIC studies obtain a stronger bound for TeV ALPs.
- It is interesting to study LBL at the CEPC and FCC-ee.



C. Baldenegro et al., JHEP06,(2018)131 (LHC LBL)
S.C. Inan and A.V. Kisselev, JHEP06(2020)183;
Chin.Phys.C 45 (2021) 4, 043109 (CLC LBL)

Searching for ALPs at future e+e- colliders via light-by-light

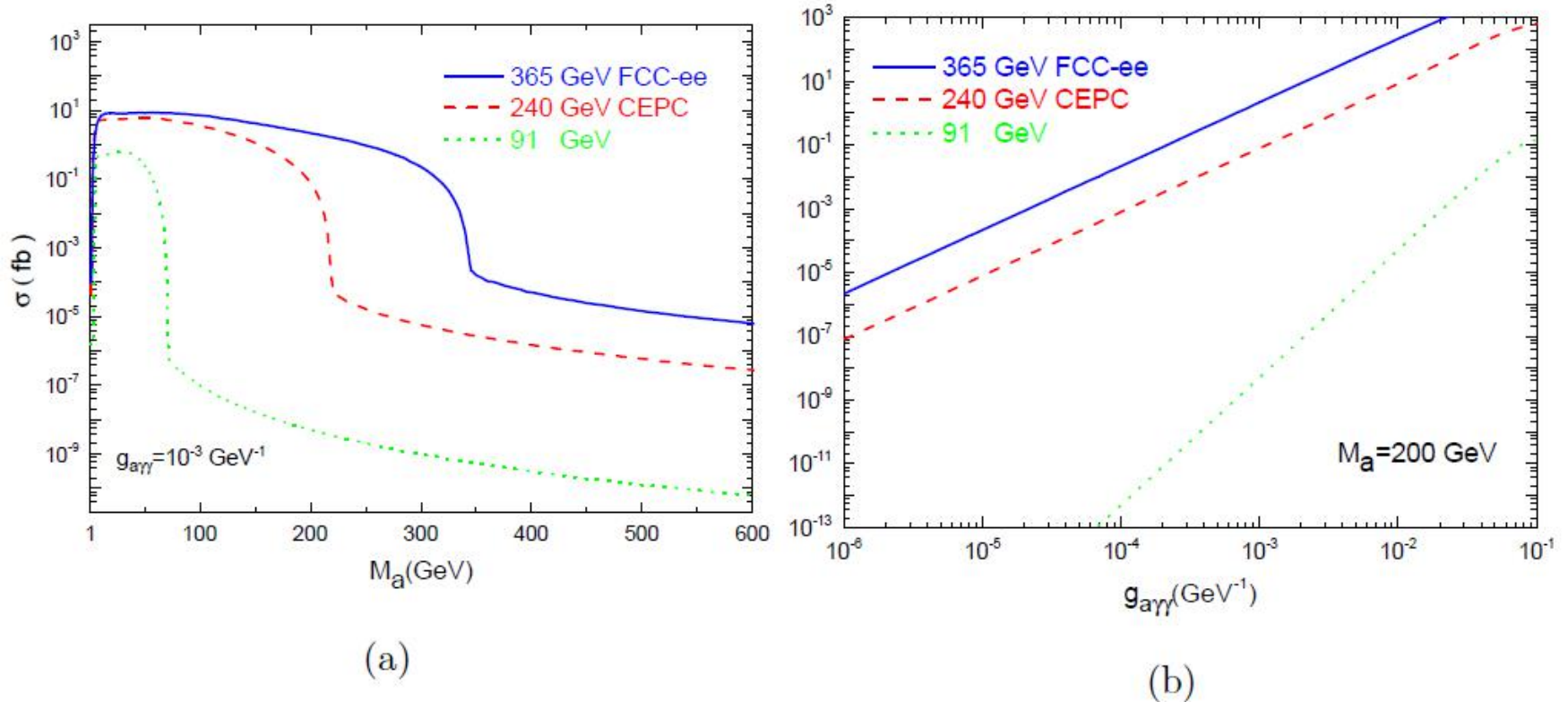


FIG. 2: The production cross section σ of the LBL scattering process induced by ALP as a function of the parameter M_a or $g_{a\gamma\gamma}$ at 365 GeV FCC-ee (blue), 240 GeV CEPC (red) and 91 GeV (green).

Background for the LBL signal

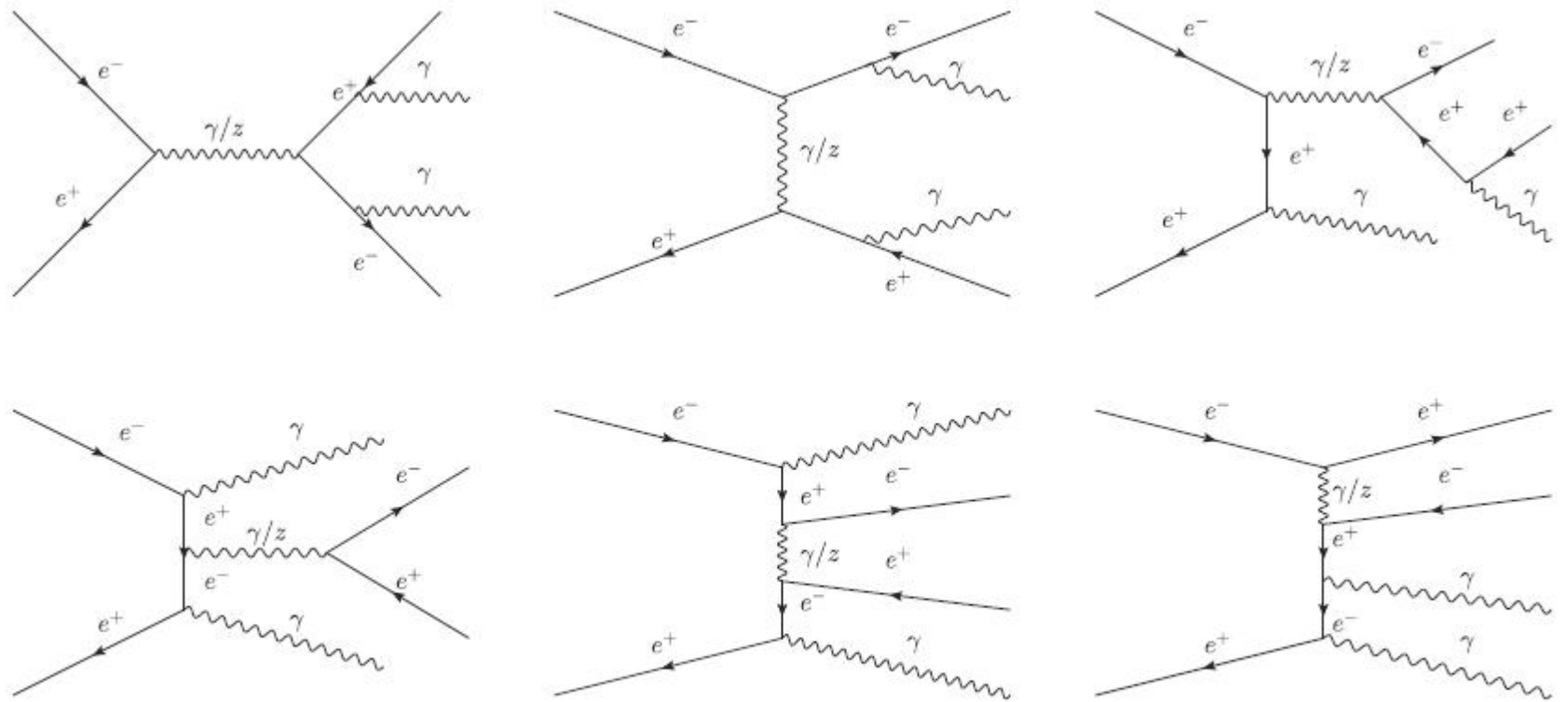


FIG. 3. The typical diagrams for the background of the process $e^+e^- \rightarrow \gamma\gamma e^+e^-$.

Detecting ALPs at the FCC-ee

Cuts	$\sqrt{s} = 365 \text{ GeV}$	$\sqrt{s} = 91 \text{ GeV}$
Cut-1: Electron and positron pseudo-rapidity	$0.6 < \eta(e^+) < 2.5$	$-0.3 < \eta(e^+) < 0.9$
	$-2.5 < \eta(e^-) < -0.6$	$-0.9 < \eta(e^-) < 0.3$
Cut-2: Angle between the ALP and the beam axis	$0.7 < \theta(\gamma\gamma) < 2.4$	$0.7 < \theta(\gamma\gamma) < 2.4$
Cut-3: Angular separation between electron-positron	$\Delta\theta(e^+e^-) < 2.9$	$\Delta\theta(e^+e^-) < 2.4$
Cut-4: Transverse momentum of reconstructed ALP	$p_T(\gamma\gamma) > 50 \text{ GeV}$	$p_T(\gamma\gamma) > 20 \text{ GeV}$

FCC-ee @ $\sqrt{s} = 365 \text{ (91) GeV}$							
Cuts	Signal (fb)						Background (fb) $\gamma\gamma e^+e^-$
	$M_a = 6 \text{ GeV}$	$M_a = 8 \text{ GeV}$	$M_a = 10 \text{ GeV}$	$M_a = 50 \text{ GeV}$	$M_a = 100 \text{ GeV}$	$M_a = 200 \text{ GeV}$	
Basic cuts	2.9092(0.2483)	5.0074(0.4786)	6.5272(0.5001)	8.4206(0.2432)	7.1235	2.1737	54.203(98.8188)
Cut 1	2.1634(0.0311)	4.2978(0.1265)	5.3419(0.142)	4.5123(0.0977)	4.9093	1.2593	29.233(41.0505)
Cut 2	1.3962(0.0307)	2.6956(0.1261)	3.6755(0.1416)	2.9963(0.0904)	3.1011	0.7942	8.3373(35.0206)
Cut 3	1.2374(0.0223)	2.5417(0.1152)	3.5173(0.1304)	2.8482 (0.0717)	2.9926	0.768	4.8137(8.4019)
Cut 4	0.9014(0.0222)	2.2243(0.115)	3.1819(0.1303)	2.5198(0.05)	2.5458	0.453	2.6445(6.1842)

Detecting ALPs at the FCC-ee

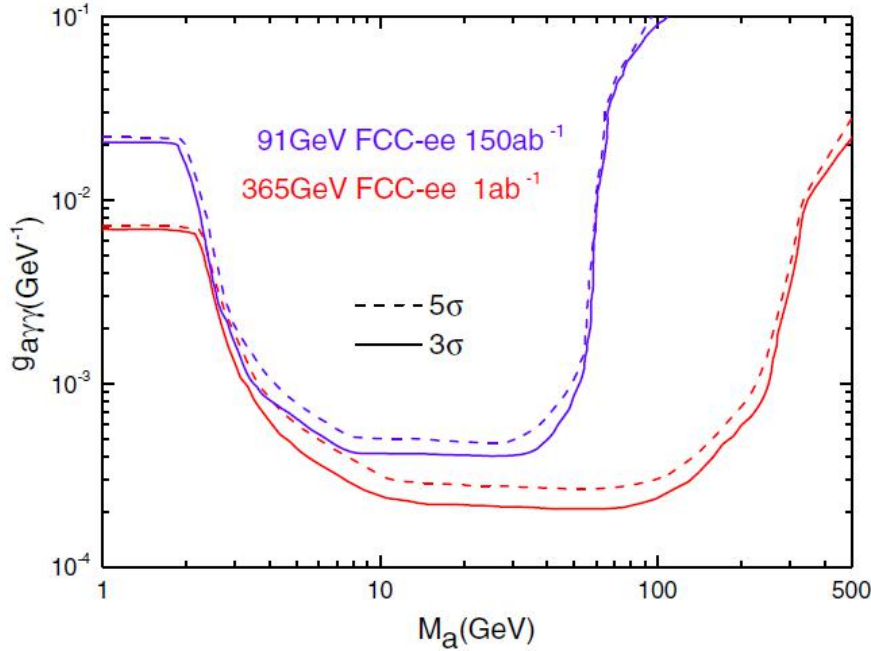


FIG. 5. The 3σ and 5σ curves in the $M_a - g_{\alpha\gamma\gamma}$ plane for $e^+e^- \rightarrow \gamma\gamma e^+e^-$ induced by ALP at 365 GeV and 91 GeV FCC-ee with the designed luminosities.

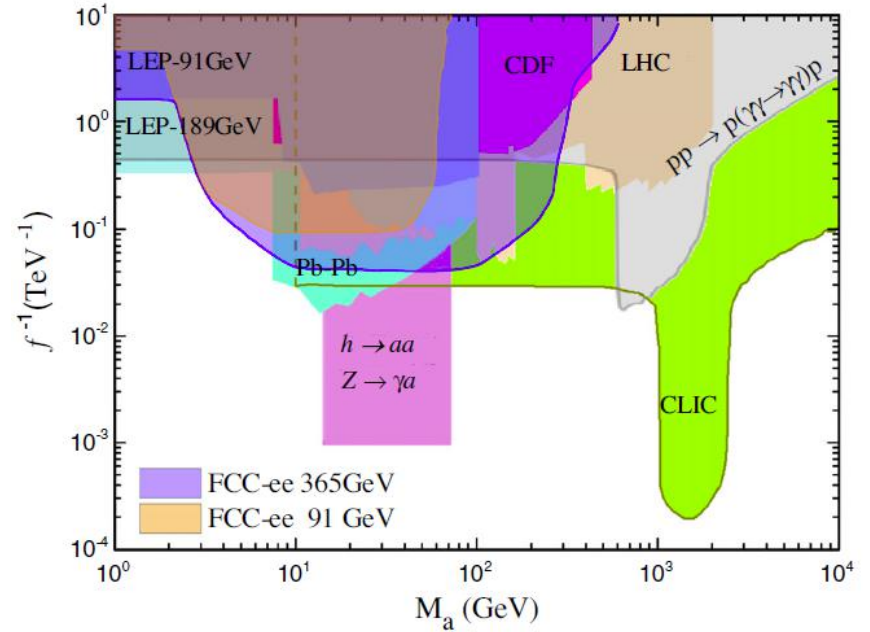


FIG. 6. The 95% C.L. exclusion regions on the ALP couplings $g_{\alpha\gamma\gamma}$ as function of M_a from the process $e^+e^- \rightarrow \gamma\gamma e^+e^-$ at FCC-ee and other current exclusion regions.

Detecting ALPs at the CEPC

Cuts	$\sqrt{s} = 240$ GeV	$\sqrt{s} = 91$ GeV
Cut-1: Electron and positron pseudo-rapidity	$0.4 < \eta(e^+) < 2.4$ $-2.4 < \eta(e^-) < -0.4$	$-0.3 < \eta(e^+) < 0.9$ $-0.9 < \eta(e^-) < 0.3$
Cut-2: Angle between the ALP and the beam axis	$0.7 < \theta(\gamma\gamma) < 2.4$	$0.7 < \theta(\gamma\gamma) < 2.4$
Cut-3: Angular separation between electron-positron	$\Delta\theta(e^+e^-) < 2.9$	$\Delta\theta(e^+e^-) < 2.4$
Cut-4: Transverse momentum of reconstructed ALP	$p_T(\gamma\gamma) > 45$ GeV	$p_T(\gamma\gamma) > 20$ GeV

CEPC @ $\sqrt{s} = 240$ (91) GeV							
Cuts	Signal (fb)						Background (fb)
	$M_a = 6$ GeV	$M_a = 8$ GeV	$M_a = 10$ GeV	$M_a = 50$ GeV	$M_a = 100$ GeV	$M_a = 160$ GeV	$\gamma\gamma e^+e^-$
Basic cuts	3.4378(0.249)	4.8088(0.4796)	5.2928(0.5003)	5.9064(0.2432)	3.585	0.8021	67.0614(98.8986)
Cut 1	2.9865(0.0316)	3.932(0.1267)	4.138(0.1417)	4.5336(0.0977)	2.4778	0.4436	33.7026(40.928)
Cut 2	2.1714(0.0309)	3.0176(0.1264)	3.2819(0.1411)	3.1262(0.0904)	1.6993	0.3145	12.628(34.93)
Cut 3	2.1368(0.0226)	3.0383(0.1156)	3.2422(0.1297)	3.0238(0.0717)	1.6497	0.3052	9.042(8.396)
Cut 4	1.4(0.0226)	2.2984(0.1156)	2.5065(0.1297)	2.0519(0.0501)	0.8747	0.0392	3.3614(6.1921)

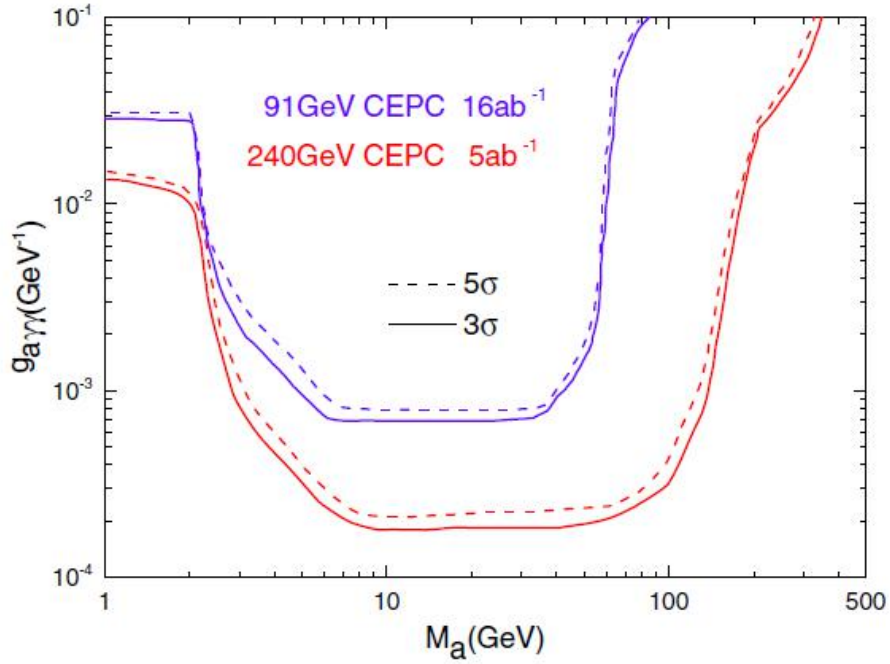


FIG. 8. The 3σ and 5σ curves in the $M_a - g_{a\gamma\gamma}$ plane for $e^+e^- \rightarrow \gamma\gamma e^+e^-$ induced by ALP at 240 GeV and 91 GeV CEPC with designed luminosities.

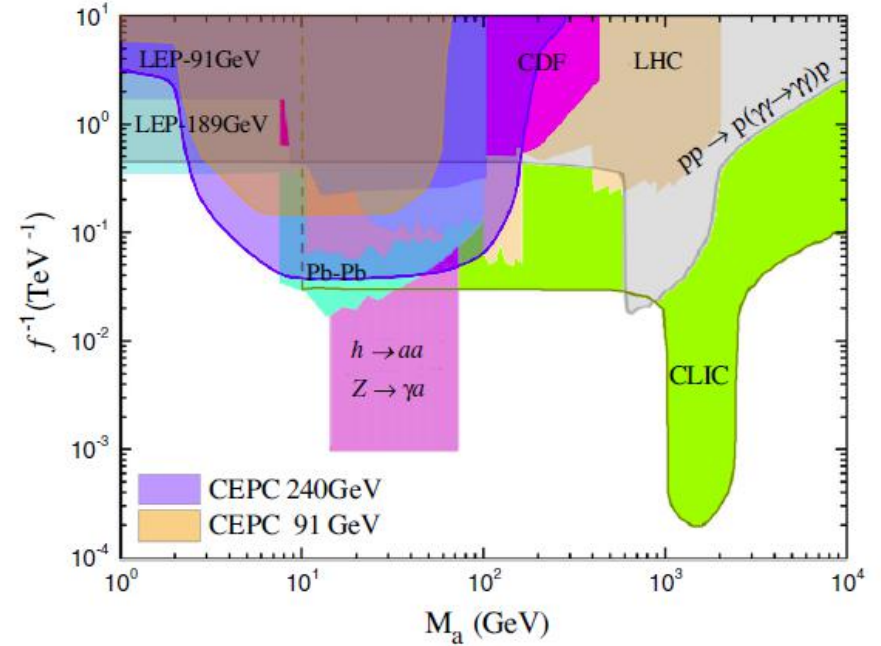


FIG. 9. The 95% C.L. exclusion regions on the ALP couplings $g_{a\gamma\gamma}$ as function of M_a from the process $e^+e^- \rightarrow \gamma\gamma e^+e^-$ at the CEPC and other current exclusion regions.

Summary

- Unlike the QCD axion, the mass and the couplings of ALPs might be independent free parameters. ALPs have a much wider parameter space and hence generate rich phenomenology at colliders.
- We have investigated the observability of the ALP diphoton signal through the light-by-light process at the FCC-ee and CEPC.
- Although the detectable mass ranges of the FCC-ee and CEPC are small, it is found that the bounds are stronger than those given by the LBL scattering at the LHC in the mass range 2~8 GeV.